COMMUNICATIONS IN SCIENCE AND TECHNOLOGY
Homepage: cst.kipmi.or.id

Effect of ratio Pluronic P123 and gelatin on titania as a catalyst in methylene blue degradation

Maria Ulfa*, Indriyani Pangestuti

Chemistry Education Study Program, Faculty of Teacher Training and Education, Sebelas Maret University, Surakarta 57126, Indonesia

Article history:
Received: 14 December 2024 / Received in revised form: 7 May 2025 / Accepted: 10 May 2025

Abstract

This study explores the influence of the gelatin-to-Pluronic P123 molar ratio on the synthesis, structural properties, and photocatalytic performance of titania for methylene blue degradation. Gelatin, employed as a biotemplate alongside Pluronic P123, effectively modulates the physicochemical characteristics of titania. As the gelatin content increases, significant changes are observed in oxygen incorporation, pore morphology, and crystallinity. Energy-dispersive X-ray spectroscopy (EDX) reveals a progressive increase in surface oxygen content from 10% (T-Gl) to 29% (T-Gh), indicating strong interactions between gelatin's NH_2 groups and titanium species. FTIR analysis confirms enhanced Ti–O–Ti bonding, with peak transmittance intensities reaching 79.857% in T-Gh. Nitrogen adsorption-desorption measurements verify mesoporosity across all samples, with pore diameters ranging from 12.4 nm to 14.8 nm and surface areas from 27.69 to 31.67 m^2/g. Crystallite sizes, determined by XRD, range between 4.27 nm and 8.56 nm, while the crystallinity varies from 45.81% to 54.55%. Despite having a lower surface area, T-Gm exhibits excellent photocatalytic efficiency (90.23%) due to favorable pore and crystallite characteristics. T-Gh demonstrates the highest performance (92.90%), attributed to its oxygen-rich surface, moderate crystallinity, and balanced mesoporous framework that enhances charge separation and dye adsorption. These findings underscore the critical role of gelatin-to-P123 ratio control in tailoring structural and surface functionalities of titania, thereby offering a sustainable strategy for designing efficient photocatalysts for environmental remediation. The developed biotemplated synthesis approach not only enhances photocatalytic performance but also promotes the use of eco-friendly and cost-effective materials, making it highly beneficial for scalable applications in wastewater treatment.

Keywords: Gelatin; Pluronic P123; titania; catalyst; methylene blue degradation

1. Introduction

Water pollution caused by dye contaminants has emerged as a critical environmental issue, especially in industrial sectors such as textiles, paper and pulp printing, rubber, plastics, cosmetics, and others, which commonly use synthetic dyes [1]. The textile industry alone consumes over 1000 tons of dye annually, with approximately 100 tons being directly discharged into water systems [2]. Synthetic dyes, including methylene blue, are preferred due to their low cost, durability, and effectiveness in coloration. However, these dyes are challenging to degrade in the environment due to their complex aromatic structure, which makes them toxic, carcinogenic, and mutagenic [3]. Their presence in water not only causes color changes and unpleasant odors but also contributes to eutrophication, oxygen depletion, and bioaccumulation, severely impacting aquatic ecosystems and human health [4]. Therefore, efficient wastewater treatment methods, such as photocatalysis, are crucial for mitigating the environmental hazards posed by these dyes.

Methylene blue, a heterocyclic aromatic cationic dye, is particularly resistant to degradation due to its stable aromatic structure, which is difficult to break down under natural conditions [5]. Traditional methods of removing dyes, such as adsorption and biological treatments, have limitations in efficiency and environmental impact. Photocatalysis, however, offers a promising solution by utilizing light energy to drive the degradation of pollutants like methylene blue into harmless substances such as water and carbon dioxide [6,7]. The effectiveness of photocatalysis depends significantly on the surface area and morphology of the photocatalyst [8]. Titanium dioxide (TiO_2) has been recognized as a leading photocatalyst due to its excellent photostability, non-toxicity, and high chemical stability, making it suitable for applications in wastewater treatment [9] However, the efficiency of TiO_2 is limited by its large band gap, which restricts its absorption to ultraviolet light, thus necessitating modifications to enhance its photocatalytic performance under visible light.

To improve TiO_2's photocatalytic properties, modifications such as the incorporation of surfactants and the creation of mesoporous structures have been explored. Mesoporous TiO_2 materials offer a higher surface area, which is essential for the adsorption of pollutants and facilitating the photocatalytic degradation process. Surfactants such as pluronic P123, a triblock copolymer, play a crucial role in forming well-ordered

* Corresponding author.
Email: ulfa.maria2015@gmail.com
https://doi.org/10.21924/cst.10.1.2025.1614

mesoporous structures and stabilizing the photocatalyst, thereby enhancing its efficiency [10,11]. Gelatin, a biopolymer with hydrophilic groups [5,12,13], has also been used as a template to further improve the surface area and porosity of TiO_2. The combination of pluronic P123 and gelatin allows for the formation of TiO_2 mesoporous materials with improved morphology, which not only enhances photocatalytic activity but also lowers the activation energy required for the degradation of methylene blue. This synergistic approach holds great potential for developing cost-effective and environmentally friendly photocatalysts for the removal of dye pollutants in wastewater treatment systems. The growing environmental concern over wastewater contamination, particularly from synthetic dyes like methylene blue, has spurred interest in the development of efficient and cost-effective photocatalytic materials [14–16]. One promising approach is the synthesis of mesoporous titanium dioxide (TiO_2) using hybrid templates such as pluronic P123, a synthetic surfactant, and gelatin, a natural biopolymer. The combination of these two surfactants in varying molar ratios offers a unique opportunity to create mesoporous TiO_2 materials with enhanced surface area, porosity, and morphological control, which are crucial for efficient photocatalytic degradation of harmful pollutants. Gelatin, being a naturally abundant and non-toxic material, presents a sustainable alternative to fully synthetic surfactants, reducing the need for complex chemical processes in the synthesis [7].

TiO_2 modification using Gelatin-Pluronic P123 combination showed significant advantages over other modification strategies in terms of morphology control, photocatalytic activity, sustainability, and application versatility. This approach utilized the synergy between protein (gelatin) and block copolymer (Pluronic P123) to create materials with improved physicochemical characteristics and superior functional performance. Gelatin, as a protein containing multiple functional groups such as $-NH_2$, -COOH, and -OH, can interact with TiO_2 surface through several mechanisms, including hydrogen bonding, electrostatic interactions, and metal coordination [17]. Meanwhile, Pluronic P123, as a trihydrate copolymer based on ethylene oxide and propylene oxide (PEO-PPO-PEO), interacted with TiO_2 precursor through its hydrophilic (PEO) and hydrophobic (PPO) moieties, forming micelle structures that guided the pore formation and morphology of nanoparticles. This interaction creates a hybrid structure that utilizes the best properties of both modifiers, resulting in better morphological control compared to other modification strategies, such as the addition of Fe metal that only forms a nanowire structure resembling a palm leaf or carbon-nitrogen doping that focuses more on the development of active metals [18]. The addition of gelatin to this system can further enhance the photocatalytic activity through several mechanisms such as increased adsorption of pollutants on the catalyst surface due to protein functional groups, better stabilization of nanoparticles and prevention of agglomeration, and sensitization of TiO_2 to visible light absorption through electron transfer from the protein chromophore [19].

This hybrid approach not only aims to improve the photocatalytic properties of TiO_2 but also aligns with the goal of minimizing the use of hazardous chemicals, thus lowering production costs, energy consumption, and environmental impact. The lack of prior research on the specific ratio of pluronic P123 and gelatin in TiO_2 mesoporous synthesis makes this study particularly relevant. By exploring the effects of different molar ratios of these surfactants, this research could lead to the development of photocatalysts that are both chemically and physically efficient while primarily relying on natural materials, paving the way for more sustainable and cost-effective wastewater treatment technologies. Research on the effect of molar ratio of gelatin to Pluronic P123 (PEO-PPO-PEO) in TiO_2 system as methylene blue degradation catalyst is a critical step in the development of high-performance photocatalytic materials. The combination of gelatin and Pluronic P123 creates a unique synergy that affects the structural properties, catalytic activity, and sustainability of the material, thus requiring ratio optimization to achieve maximum performance [20-22].

2. Materials and Methods

2.1. Material

The materials used in this study include 37% HCl from Sigma-Aldrich Merck KGaA (Molar Mass: 0.0365 kg/mol), commercial gelatin from Gelita (Molar Mass: 90 kg/mol), Tetraethyl orthotitanate (TEOT) from Sigma-Aldrich Merck KGaA (Molar Mass: 0.2281 kg/mol), Pluronic P123 from Sigma-Aldrich Merck KGaA (Molar Mass: 5.8 kg/mol), ethanol from Sigma-Aldrich Merck KGaA (Molar Mass: 0.0461 kg/mol), and Methylene Blue from Sigma-Aldrich Merck KGaA (Molar Mass: 0.3199 kg/mol).

2.2. Synthesis Mesoporous TiO_2 modified with gelatin

In the synthesis of mesoporous TiO_2 modified with gelatin at varying molar ratios, the following procedure is carried out for each formulation: For the first formulation, the molar ratio of gelatin to Pluronic P123 is 1:33, labeled as T-Gl, representing TiO_2 synthesized with a low gelatin content. For the second formulation, the molar ratio of gelatin to Pluronic P123 is 1:16, labeled as T-Gm. The third formulation, with a gelatin to Pluronic P123 ratio of 1:7, is labeled as T-Gh. Each formulation involves dissolving the appropriate moles of gelatin and Pluronic P123 in ethanol (61 mL) in a beaker. After mixing and dissolving, hydrochloric acid (HCl) is prepared by diluting 10.66 mL of concentrated HCl with 69 mL of deionized water. The HCl solution is slowly added to the surfactant mixture and stirred for 1 hour at 40°C at a speed of 500 rpm. Tetraethyl orthotitanate (TEOT) is then added dropwise, and the mixture is stirred for 24 hours under the same conditions. Afterward, the mixture is transferred to a 250 mL hydrothermal autoclave for aging at 90°C for 24 hours. Finally, the resulting precipitate is filtered and dried in an oven at 70°C for 24 hours, followed by calcination at 550°C for 5 hours to obtain the TiO_2 powder with the corresponding gelatin: Pluronic P123 molar ratios for each formulation (T-Gl, T-Gm, T-Gh).

The selection of molar ratios 1:33, 1:16, and 1:7 for gelatin to P123 in this study was guided by trends observed in previous research that employed both synthetic and natural surfactants in mesoporous TiO_2 synthesis. As shown in Table 1, earlier

studies have used a wide range of ratios depending on the nature and interaction strength of the co-surfactants. For instance, combinations like CTAB/P123 ranged from 1:1 to 1:10 [22], gum arabic:P123 from 1:0 to 1:25 [23], and rose petal extract:P123 from 1:20 to 1:40 [24]. These variations highlight the need for ratio optimization based on the specific physicochemical behavior of the natural template involved. Therefore, the ratios used in this work were chosen to cover a broad spectrum from low to high gelatin content, enabling the evaluation of its influence on mesostructure formation, porosity control, and photocatalytic efficiency. This gradient approach allows for systematic insight into the synergistic role of gelatin as a natural biotemplate in comparison to literature-based benchmarks.

Table 1. Comparison of surfactant ratios used in mesoporous TiO_2 synthesis

Ratio	Surfactant
1:1 -1:10	CTAB/P123[22]
1:0- 1:25	gum arabic:P123[23]
1:20 -1:40	rose petal:P123 [24]
1:33, 1:16, 1:7	Gelatin :P123 [This work]

2.3. Characterization

The instruments used for characterizing the samples in this study include X-Ray Diffraction (XRD) from Panalytical (Model PW3050/60), operated within a 2θ range of 5° to 80°, to determine the crystallinity and phase composition of the synthesized materials. The surface area and porosity were measured using the Brunauer-Emmett-Teller (BET) method with a Quantachrome Nova 1200e instrument. Fourier Transform Infrared Spectroscopy (FTIR), performed using a Shimadzu 21 spectrometer with a resolution of 0.5 cm^-1, was employed to analyze functional groups in the materials in the wavenumber range of 300–4000 cm^{-1}. Scanning Electron Microscopy with Energy Dispersive X-Ray (SEM-EDX) analysis was conducted using a JEOL JSM-700 microscope at a voltage of 15 kV to observe the surface morphology and elemental composition of the samples. Transmission Electron Microscopy (TEM) was carried out at 120 kV to investigate the internal structure of the mesoporous TiO_2 materials. Additionally, Differential Thermal Analysis (DTA) and Thermogravimetric Analysis (TGA) were used to study the thermal stability and composition of the samples.

2.4. Photodegradation

To carry out the photocatalytic degradation process, a 200 mL solution of Methylene Blue at a concentration of 30 ppm is prepared. This solution is then poured into an Erlenmeyer flask and placed inside a photocatalytic reactor. Subsequently, 20 mg of mesoporous TiO_2 photocatalyst is added to the Methylene Blue solution in the Erlenmeyer. The adsorption process is initiated by shaking the flask in the dark within the reactor for 60 minutes. After adsorption, the Methylene Blue solution is transferred into ten 10 mL dark glass vials inside the photocatalytic reactor under dark conditions. One vial is labeled as "Co," indicating the initial concentration before photocatalytic treatment (i.e., at 0 minutes). The remaining nine vials are placed on a shaker within the reactor, ensuring they remain in the dark without caps. The photocatalytic degradation begins by activating the UV lamp and the shaker to initiate the process.

3. Results and Discussion

3.1. XRD

Based on the XRD patterns shown in Fig. 1, the diffraction peaks observed in all samples (T-Gl, T-Gm, and T-Gh) confirm the presence of both anatase and rutile phases of TiO_2, as identified by their characteristic peaks in reference to JCPDS cards 21-1272 (anatase) and 21-1276 (rutile) [25]. Notably, the T-Gl sample exhibits dominant peaks corresponding to the anatase phase, particularly at $2\theta \approx 25.3°$, which aligns with the main anatase (101) reflection.

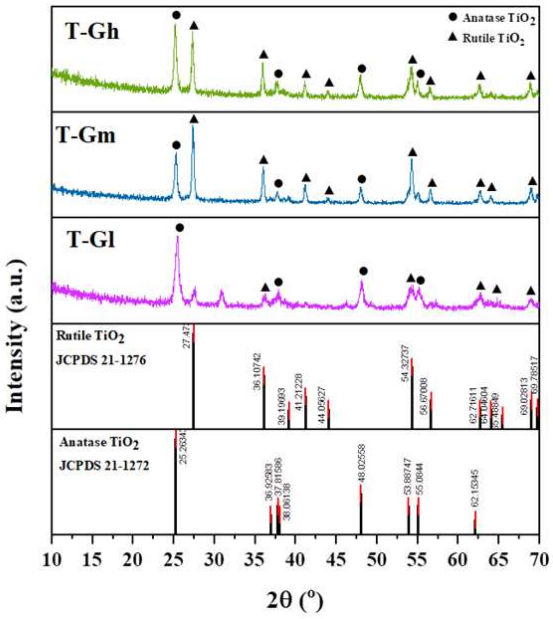

Fig. 1. XRD of titania: T-Gl (low gelatin); T-Gm (medium gelatin); T-Gh (high gelatin) concentration

However, as the gelatin concentration increases (in T-Gm and T-Gh), the intensity of the rutile peaks, especially those at $2\theta \approx 27.4°$ (rutile (110)), becomes more prominent, indicating a phase transformation from anatase to rutile. This trend suggests that higher gelatin content may facilitate rutile phase formation, possibly due to changes in the thermal behavior or microstructural evolution during synthesis. Therefore, the XRD results clearly demonstrate a shift in the dominant TiO_2 phase from anatase in T-Gl to rutile in T-Gh. Further details are provided in Table 2

Table 2 presents a comparative analysis of the crystallographic properties of TiO_2 synthesized in this study alongside standard JCPDS data and previous literature utilizing Pluronic P123 as a templating agent. The TiO_2 samples obtained in this study exhibited both anatase and rutile phases, with dominant diffraction peaks observed at $2\theta = 25.3°$ and 27.4°, respectively, consistent with JCPDS No. 21-1272 (anatase) and 21-1276 (rutile). Crystallite sizes calculated via the Scherrer equation were 12.5 nm for anatase and 18.7 nm for rutile, indicating nanoscale crystallinity. Comparatively,

literature sources using P123 reported predominantly anatase phases with crystallite sizes ranging from approximately 5 to 15 nm, indicating that the templating agent and synthesis conditions significantly influence the development of TiO_2 crystallites and phase formation. This comparison supports the reproducibility of anatase phase generation using P123 and highlights the variation introduced by synthesis parameters.

Table 2. comparative crystallographic data of TiO_2 samples

Sample Description	Crystal Phase	Dominant 2θ Peak (°)	Crystallite Size (nm)	Reference
TiO_2	Anatase	25.3	12.5	This work
TiO_2	Rutile	27.4	18.7	This work
TiO_2 (JCPDS No. 21-1272)	Anatase	25.3	—	JCPDS Standard
TiO_2 (JCPDS No. 21-1276)	Rutile	27.4	—	JCPDS Standard
TiO_2 synthesized with P123	Anatase	25.3	10–15	[19]
TiO_2 synthesized with P123	Anatase	25.3	~5.1	[21,26]
TiO_2 synthesized with Pluronic P123	Anatase	25.3	~9.8	[24]

Rutile phase does not appear in the Gelatin-Pluronic P123 integrated TiO_2 photocatalyst due to the combination of synthesis factors and anatase phase stabilization mechanism by this biotemplate system. Gelatin forms a cross-linking network with Fe^{3+} ions that enhances the thermal stability of the anatase phase up to 700°C. This prevents the transformation of the anatase phase to rutile which usually occurs at 600-800°C [27-29]. Pluronic P123 forms micelles that direct the growth of TiO_2 crystals through the restriction of growth space by the hydrophobic PPO chains, selective interaction with the anatase crystal surface (Miller101 index), and inhibition of Ti^{4+} ion diffusion required for rutile crystal reorganization. Synthesis conditions with Gelatin-P123 include low calcination temperature (450-550°C vs >600°C for conventional synthesis), short crystallization time (2-4 h vs 12-24 h), and neutral pH (6.8-7.2) which does not support rutile formation [24-25].

3.2. BET

Fig. 2 shows the adsorption-desorption isotherms of three samples (T-Gh, T-Gm, and T-Gl), which correspond to the synthesis of titania using different concentrations of gelatin. The isotherms for all three samples follow Type IV of the IUPAC classification [30], which is typically associated with mesoporous materials. This indicates the presence of mesopores in all three samples, suggesting that the titania formed exhibits mesoporous characteristics. Although there are differences in the gelatin concentrations used (low to high), the isotherms do not show significant changes, implying that the overall porosity type remains consistent across the samples. However, there are differences in the pore size distribution. The shift in pore size, from the lower gelatin concentration to the higher gelatin concentration, results in an increase in the average pore size. Specifically, the pore radius increases from 62 Å in the sample with lower gelatin (T-Gl) to 74 Å in the sample with higher gelatin (T-Gh).This increase in pore size may be attributed to the influence of gelatin concentration on the structural evolution of the TiO_2 framework, where higher amounts of gelatin may lead to more expanded pore structures. The condensation process during calcination, influenced by the organic template, could contribute to the stabilization and growth of larger mesopores. Additionally, the calcination process effectively decomposes the gelatin, further affecting the final structure of the titania.

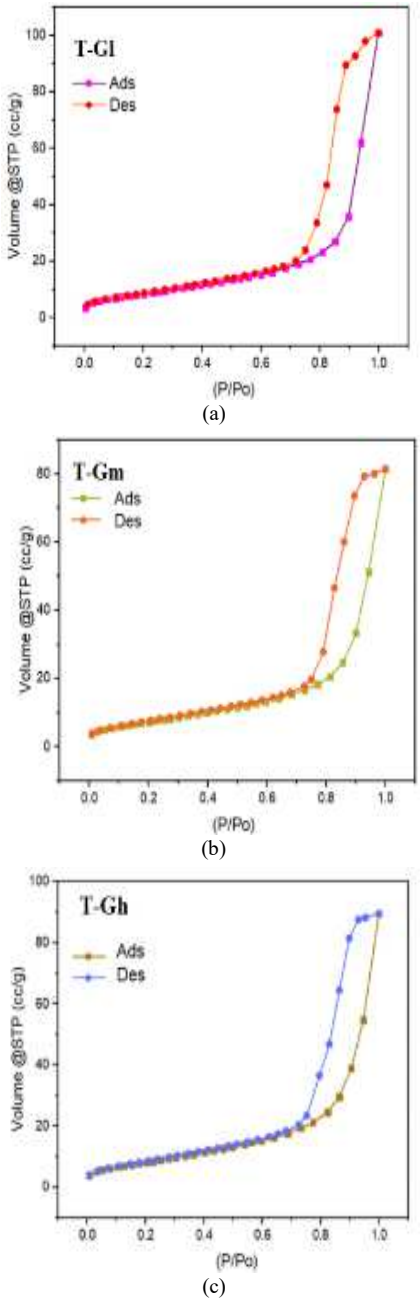

Fig. 2. Isotherm adsorption-desorption of Titania : (a) T-Gl (Low gelatin); (b) T-Gm (Medium gelatin); (c) T-Gh (High gelatin) concentration

Table 3. Peak radius and corresponding pore diameter of TiO_2 samples synthesized with varying gelatin concentration

Sample	Peak Radius (Å)	Pore Diameter (Å)	Pore Diameter (nm)
T-Gl	~62 Å	~124 Å	12.4 nm
T-Gm	~68 Å	~136 Å	13.6 nm
T-Gh	~74 Å	~148 Å	14.8 nm

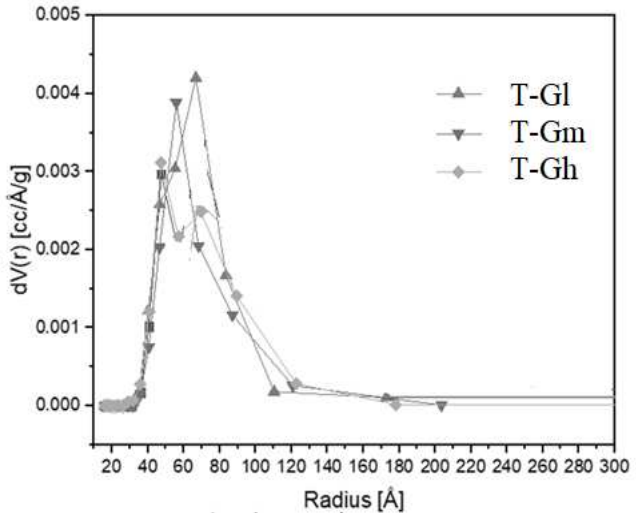

Fig. 3. Pore size distribution of titania of T-Gl (low gelatin); T-Gm (medium gelatin); T-Gh (high gelatin) concentration

Table 4. Comparison of isotherm type and pore diameter of bare and gelatin-modified TiO_2 samples

Sample Description	Isotherm Type	Average Pore Diameter (nm)	Reference
T-Gl (Low gelatin concentration)	Type IV (IUPAC)	12.40	This work
T-Gm (Medium gelatin concentration)	Type IV (IUPAC)	13.60	This work
T-Gh (High gelatin concentration)	Type IV (IUPAC)	14.8	This work
Bare TiO_2 (Sol-Gel method)	Type IV (IUPAC)	14.3	[31]
TiO_2 (P123 template)	Type IV (IUPAC)	10.5	[1]
TiO_2 (Nanoparticles, Hydrothermal)	Type IV (IUPAC)	12.1	[32]

Table 4 presents a comparative analysis of the isotherm types and average pore diameters of TiO_2 samples synthesized through various methods, including both bare TiO_2 and gelatin-modified TiO_2. All samples, including those synthesized with low, medium, and high gelatin concentrations (T-Gl, T-Gm, T-Gh), exhibit Type IV isotherms according to the IUPAC classification, indicating the presence of mesoporosity in all the materials. The average pore diameter of the bare TiO_2 sample synthesized using the hydrothermal method is 13.78 nm, while the pore diameter of the gelatin-modified samples increases progressively from 12.4 nm (T-Gl) to 14.8 nm (T-Gh), highlighting the influence of gelatin concentration on the mesoporous structure of TiO_2. The table also includes data from other studies, showing a pore diameter of 14.3 nm for TiO_2 synthesized via the sol-gel method, 10.5 nm for TiO_2 templated with Pluronic P123, and 12.1 nm for hydrothermally synthesized TiO_2 nanoparticles. These results collectively demonstrate that gelatin modification plays a significant role in tuning the pore structure of TiO_2, contributing to the overall mesoporosity and pore size control.

Although the specific surface area does not show significant differences, the variation in pore size may occur due to changes in nanoparticle morphology during the synthesis process. The formation process of TiO_2 can cause the coalescence or widening of existing pores, thereby affecting the average pore size without drastically impacting the total surface area [33]. The hydrothermal process can produce nanoparticles with different size distributions. The variation in particle packing may influence the space between them, thereby modifying the pore size without significantly changing the surface area [34]. During calcination, TiO_2 particles can undergo consolidation or expansion, resulting in changes in pore size, although the surface area remains relatively stable. The anatase phase of TiO_2 has a crystal structure that affects the adsorption properties. The anatase phase is more dominant and evenly distributed, thus producing a stable surface area despite changes in pore size [35,36].

3.3. FTIR

The FTIR spectra (Fig. 4) of the synthesized titania samples (T-Gh, T-Gm, and T-GI) show distinct absorption bands in the range of 400–500 cm^{-1}, which are attributed to Ti–O–Ti bonding vibrations [36]. This is evident from the prominent peaks observed at 498.35 cm^{-1} for T-Gl, 491.43 cm^{-1} for T-Gm, and a broader response with peaks at 411.03 and 500.64 cm^{-1} for T-Gh. These features are characteristic of titanium dioxide (TiO_2) and confirm the successful formation of a titanium–oxygen framework in the synthesized materials. Additionally, the presence of water molecules is supported by broad absorption bands in the higher wavenumber region, notably around 1600 cm^{-1}, which are likely due to adsorbed water during storage. The Ti–O–Ti bands affirm the development of a titanium–oxide network, consistent with previous reports on TiO_2 synthesized from various precursors, including gelatin.

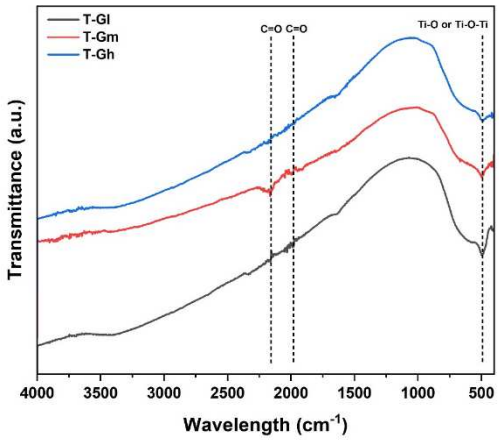

Fig. 4. FTIR of titania of T-Gl (low gelatin); T-Gm (medium gelatin); T-Gh (high gelatin) concentration

Although the Fig. 4 and Table 5 do not specifically detail the differences in gelatin ratios, variations among the samples can be inferred through the peak areas associated with Ti–OH, Ti–O, and Ti–O–Ti functional groups. These distinctions are observed in the subtle changes in peak intensity and area. Notably, with increased gelatin content, there is a small but observable shift and variation in the transmittance values and positions, particularly within the Ti–O and Ti–O–Ti region (~400–800 cm^{-1}). This suggests modifications in the titanium bonding environment. Additionally, the presence or relative decrease in Ti–OH-related regions—typically seen around ~3300–3700 cm^{-1}—implies structural adjustments within the material as gelatin concentration changes.

Table 5. Extracted Peak Positions and Intensities of all sample

Sample	Peak Position (cm^{-1})	Intensity (%T)	Functional Group (Tentative)
T-Gl	498.35	70.836	Ti–O or Ti–O–Ti
T-Gm	491.43	72.327	Ti–O or Ti–O–Ti
T-Gh	411.03, 500.64	79.857, 76.786	Ti–O or Ti–O–Ti
	1993.36, 2163.97	77.504, 71.046	Possibly C=O / surface group

Quantitatively, the Ti–O–Ti region shows a progressive increase in transmittance with higher gelatin content, from 70.836% in T-Gl, to 72.327% in T-Gm, and reaching 76.786% and 79.857% in T-Gh. This reflects an approximate 8.5% increase in intensity from T-Gl to T-Gh, indicating enhanced network formation of Ti–O–Ti bonds in the presence of more gelatin. Such differences suggest a more developed titania framework as the templating effect of gelatin increases. These observations align with changes in the functional group distributions, reflecting that the gelatin amount does indeed influence the material's internal structure and contributes to the successful incorporation and templating of titania during synthesis.

3.4. SEM

The SEM results indicate that the presence of gelatin as a template in the titania synthesis leads to the expansion of the agglomerate size. As the amount of gelatin increases, the interaction between the amino groups (NH_2) in the gelatin and the titania matrix intensifies. This is due to the higher electronegativity of nitrogen (3.04) in the amino group compared to titanium (1.54) [37], which enhances the affinity of the amino groups toward titania. This interaction promotes stronger aggregation of the titania particles, resulting in larger agglomerates.

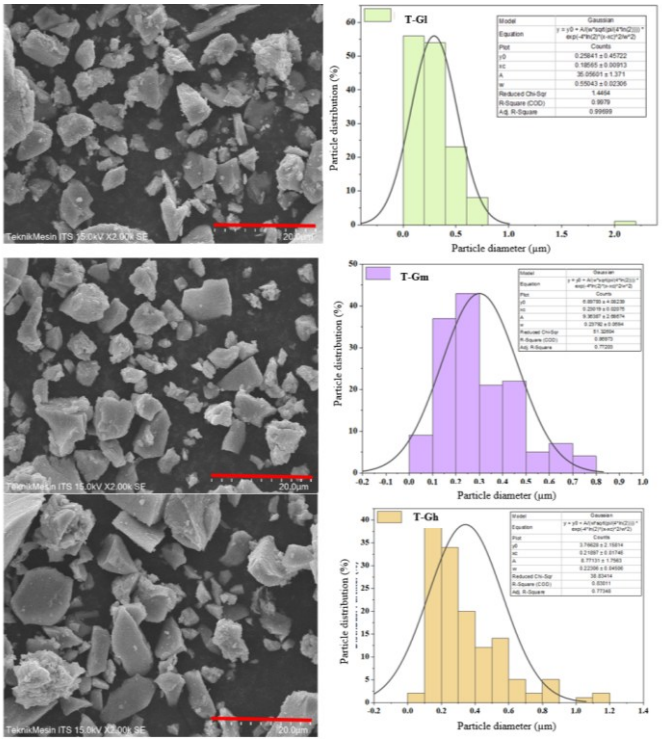

Fig. 5. SEM of Titania of T-Gl (low gelatin); T-Gm (medium gelatin); T-Gh (high gelatin) concentration

The histograms clearly show a shift towards larger particle sizes as the gelatin concentration increases, corroborating the increased agglomeration. The interaction between the highly electronegative nitrogen in the amino groups and the titanium surface facilitates a stronger pull, causing significant aggregation of titania particles. This effect demonstrates the critical role of gelatin not only as a template but also in enhancing particle clustering through electrostatic interactionbetween the nitrogen and titanium atoms.

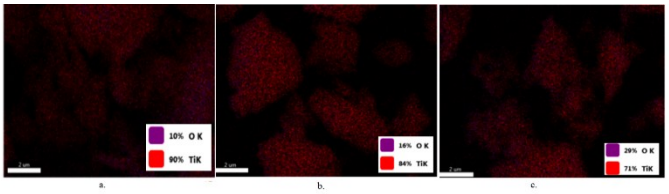

Fig. 6. SEM EDX of Titania of T-Gl (low gelatin); T-Gm (medium gelatin); T-Gh (high gelatin) concentration

The data reveals a strong correlation between the structural properties of the titania samples and their photocatalytic performance in photodegradation. Specifically, the Ti-Gl and Ti-Gh samples exhibit relatively higher surface areas (~31.7 m^2/g) compared to Ti-Gm (27.7 m^2/g), which generally supports enhanced photocatalytic activity by increasing the availability of active surface sites. Interestingly, Ti-Gm, despite having the lowest surface area, still demonstrates a high photodegradation efficiency (90.23%), indicating the contribution of other structural parameters.

In terms of porosity, all samples display mesoporous characteristics, with pore diameters ranging from 12.4 to 14.8 nm. T-Gm shows the largest pore diameter (13.6 nm), followed closely by T-Gh (14.8 nm) and T-Gl (12.4 nm). These differences in pore size influence the balance between reactant accessibility and charge separation. Ti-Gl, with the smallest pore diameter, may offer more confined diffusion environments, whereas Ti-Gh, with the largest pore diameter and optimal surface area, appears to provide improved charge carrier mobility and enhanced interaction with dye molecules. This structural synergy likely underlies Ti-Gh's superior photodegradation efficiency of 92.90%, as it supports both effective charge separation and efficient molecular diffusion. Thus, the combination of surface area and mesopore architecture—reflected by the increasing peak radius (from ~62 Å in T-Gl to ~74 Å in T-Gh)—plays a pivotal role in tuning the photocatalytic performance of these gelatin-modified titania materials.

The crystallite size and crystallinity further highlight the interplay of structural parameters. Ti-Gm has the largest crystallite size (8.56 nm) but the lowest crystallinity (45.81%), which can hinder charge transport and light absorption. On the other hand, Ti-Gh, with its intermediate crystallite size (6.89 nm) and moderate crystallinity (51.32%), achieves a balance that enhances photocatalytic performance. The reduced crystallite size minimizes the recombination of photogenerated electron-hole pairs, while sufficient crystallinity supports effective light harvesting. Aggregate size, which increases with gelatin concentration, also influences performance. Although Ti-Gh has the largest aggregates (0.342 μm), the smaller crystallite size and favorable mesoporous structure compensate for any limitations in light penetration. The superior performance of Ti-Gh can be attributed to its optimized

combination of physical and chemical properties. Its higher oxygen content (29%), moderate crystallinity (51.32%), and mesoporous framework (14.8 nm pore diameter, 31.37 m²/g surface area) synergistically enhance photocatalytic efficiency (92.90%) by facilitating reactant interactions and reducing electron-hole recombination.

Table 6. porosity and photodegradation data for TiO_2 samples

Sample Type	Ti-Gl	Ti-Gm	Ti-Gh	Bare TiO_2 (Hydrothermal)	Bare TiO_2 (Sol-Gel)	TiO_2 (Pluronic P123)
Surface Area (BET, m²/g)	31.669	27.690	31.371	55.0	62.0	47.0
Total Pore Volume (cc/g)	0.1561	0.1261	0.1386	0.220	0.250	0.180
Pore Diameter (BJH desorption method, nm)	12.40	13.60	14,80	15.0	12.5	10.0
Mesopore Surface Area (m²/g)	31.669	27.690	31.371	55.0	62.0	47.0
Mesopore Volume (cc/g)	0.167	0.133	0.144	0.180	0.210	0.160
Aglomerate Diameter by EDX (μm)	0.293	0.300	0.342	0.280	0.260	0.275
Crystallite Size by XRD (nm)	4.27	8.56	6.89	9.5	12.0	8.0
Crystallinity by XRD (%)	54.55	45.81	51.32	72.0	78.0	68.0
Ti (%w/w) by EDX	90	84	71	98	99	96
O (%w/w) by EDX	10	16	29	2	1	4
Efficiency of Photodegradation (%)	87.23	90.23	92.90	85	82	88
References	This work			[38]	[39]	[9]

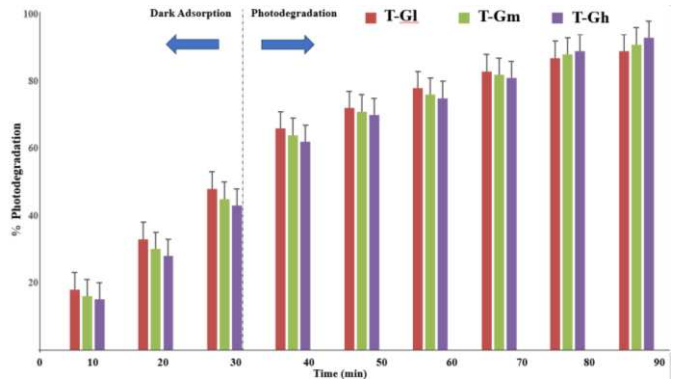

Fig. 7. Photodegaradtion of titania of T-Gl (low gelatin); T-Gm (medium gelatin); T-Gh (high gelatin) concentration

Gelatin-Pluronic P123 templating plays a significant role in enhancing the photocatalytic performance of TiO_2, especially in terms of charge separation and reduction of electron-hole recombination. This mechanism is explained by several interrelated aspects. Gelatin-P123 acts as a structure-directing agent, creating high porosity and uniform pore distribution. This increases the number of active sites for photocatalytic reactions and facilitates oxygen and pollutant diffusion. The regular mesoporous structure (12.4–14.8 nm) minimizes the migration distance between electrons and holes, reducing recombination [40].Furthermore, this templating stabilizes the anatase phase by preventing agglomeration and phase transformation. Gelatin's -NH_2 and -COOH groups chemically bind to the TiO_2 surface, forming electron traps that delay recombination. Pluronic P123 also contributes to anatase crystal quality, improving charge transfer efficiency[41]

Additionally, gelatin functions as a visible light sensitizer due to chromophore groups that absorb visible light and transfer energy to TiO_2's conduction band. This extends activity into the visible spectrum. The charge redistribution by Pluronic P123 creates a microenvironment with separated hydrophilic and hydrophobic zones. Hydrophilic zones adsorb water and oxygen, while hydrophobic regions assist organic pollutant diffusion. This structural separation keeps electron-hole pairs apart until they reach reaction sites. Thus, the combination of mesoporosity, anatase stabilization, recombination suppression, and sensitization boosts activity under UV and visible light [42,43].

The gelatin concentration during Ti-Gl, Ti-Gm, and Ti-Gh synthesis significantly influences the oxygen content and structural morphology, as confirmed by EDX and BET analyses. The oxygen content increases with higher gelatin ratios: 10% (Ti-Gl), 16% (Ti-Gm), and 29% (Ti-Gh), while Ti content decreases accordingly from 90% to 84% to 71%. This oxygen increment enhances MB adsorption during dark conditions and contributes to efficient photodegradation upon irradiation. Higher oxygen content improves active site interactions with methylene blue, increasing breakdown efficiency into CO_2 and H_2O. The increased pore diameter from 12.4 nm (Ti-Gl) to 13.6 nm (Ti-Gm) and 14.8 nm (Ti-Gh) also improves reactant transport.

Despite Ti-Gm having the lowest surface area (27.69 m²/g), its efficiency (90.23%) remains high due to optimized crystallite size and porosity. Ti-Gh outperforms all samples (92.90%) due to its oxygen-rich surface, moderate crystallinity, and mesoporous structure. These results emphasize the importance of gelatin-to-P123 ratio control in tuning titania's structure, surface chemistry, and photocatalytic function for environmental remediation applications.

4. Conclusion

This study demonstrates that the gelatin-to-Pluronic P123 molar ratio significantly influences the physicochemical and photocatalytic characteristics of titania synthesized for methylene blue degradation. As the gelatin content increases from T-Gl to T-Gh, EDX analysis reveals a notable rise in surface oxygen content—from 10% to 29%—indicating enhanced oxygen incorporation due to strong coordination between gelatin's amino groups and titanium species. FTIR spectra support this with increased Ti–O–Ti band intensity, notably reaching 79.857% transmittance in T-Gh. All samples exhibit mesoporous structures, with pore diameters expanding from 12.4 nm (T-Gl) to 14.8 nm (T-Gh), which facilitate

efficient dye molecule diffusion and product desorption. Although T-Gm has the lowest surface area (27.69 m^2/g), it maintains high degradation efficiency (90.23%) due to larger pore size and higher crystallite size (8.56 nm). T-Gh, with balanced properties—oxygen-rich surface, moderate crystallinity (51.32%), and mesopore volume of 0.144 cc/gachieved the highest photocatalytic performance (92.90%). These results confirm that precise tuning of the gelatin-to-P123 ratio enables structural optimization, improving charge separation, adsorption capacity, and reactivity, thus making gelatin-modified titania a promising photocatalyst for environmental remediation applications.

Acknowledgements

Manuscripts The authors express their heartfelt gratitude to Universitas Sebelas Maret (UNS) for their financial support through Penelitian Unggulan Terapan- A (PUTA)(369/UN27.22/PT.01.03/2025). This support has been instrumental in facilitating the successful completion of this research. The authors also appreciate the resources and opportunities provided, which significantly contributed to the quality and impact of this study.

References

1. *Synthesis and characterisation of mesoporous anatase TiO2 with highly crystalline framework*. 2013.
2. P.K. Jaseela, J. Garvasis and A. Joseph, *Selective Adsorption Of Methylene Blue (Mb) Dye From Aqueous Mixture Of Mb And Methyl Orange (Mo) Using Mesoporous Titania (Tio2) – Poly Vinyl Alcohol (Pva) Nanocomposite*, J. Mol. Liq. 286 (2019), pp. 110908.
3. W.K. Essa, S.A. Yasin, A.H. Abdullah, M.R. Thalji, I.A. Saeed, M.A. Assiri et al., *Polyethylene Terephthalate Nanofiber-Multi-Walled Carbon Nanotube Composite*, Water 25 (2022).
4. L. Usgodaarachchi, C. Thambiliyagodage, R. Wijesekera and M.G. Bakker, *Synthesis of mesoporous silica nanoparticles derived from rice husk and surface-controlled amine functionalization for efficient adsorption of methylene blue from aqueous solution*, Curr. Res. Green Sustain. Chem. 4 (2021).
5. M. Ulfa and I. Setiarini, *The Effect of Zinc Oxide Supported on Gelatin Mesoporous Silica (GSBA-15) on Structural Character and Their Methylene Blue Photodegradation Performance*, Bull. Chem. React. Eng. Catal. 17 (2022), pp. 363–374.
6. M. Ulfa, H. Al Afif, T.E. Saraswati and H. Bahruji, *Fast Removal of Methylene Blue via Adsorption-Photodegradation on TiO2/SBA-15 Synthesized by Slow Calcination*, Materials (Basel). 15 (2022), pp. 1–13.
7. M. Ulfa, D. Prasetyoko, H. Bahruji and R.E. Nugraha, *Pluronic F127-Gelatin Template for Adsorption and Photodegradation of Ibuprofen*, (2021).
8. M. Tuna, G. Yanalak, G. Arslan and I. Hatay, *Materials Science in Semiconductor Processing Green preparation of Carbon Quantum dots using Gingko biloba to sensitize TiO 2 for the photohydrogen production*, Mater. Sci. Semicond. Process. 109 (2020), pp. 104945.
9. A. Mancuso, O. Sacco, V. Vaiano, B. Bonelli, S. Esposito, F.S. Freyria et al., *Visible light-driven photocatalytic activity and kinetics of fe-doped tio<inf>2</inf> prepared by a three-block copolymer templating approach*, Materials (Basel). 14 (2021).
10. J. Górka, C. Fenning and M. Jaroniec, *Influence of temperature, carbon precursor/copolymer ratio and acid concentration on adsorption and structural properties of mesoporous carbons prepared by soft-templating*, Colloids Surfaces A Physicochem. Eng. Asp. 352 (2009), pp. 113–117.
11. M. Jaroniec, J. Gorka, J. Choma and A. Zawislak, *Synthesis and properties of mesoporous carbons with high loadings of inorganic species*, Carbon N. Y. 47 (2009), pp. 3034–3040.
12. M. Ulfa, D. Prasetyoko and H. Bahruji, *Hexagonal Flake- Like Hematite (α -Fe 2 O 3) Prepared by Hybrid Pluronic F127-Gelatin as Eco-Friendly Template for Adsorption of Ibuprofen*, (2021), pp. 1–15.
13. R.H. John Korthrop and M. Kusitz, *Swelling Bxd Hydration of Gelatixi*, J. Phys. Chem. 35 (1930) 162–184.
14. A. V. Nakhate and G.D. Yadav, *Cu2O nanoparticles supported hydrothermal carbon microspheres as catalyst for propargylamine synthesis*, Mol. Catal. 451 (2018), pp. 209–219.
15. M. Ulfa, D. Prasetyoko, W. Trisunaryanti, H. Bahruji, Z.A. Fadila and N.A. Sholeha, *The effect of gelatin as pore expander in green synthesis mesoporous silica for methylene blue adsorption*, Sci. Rep. 12 (2022), pp. 1–12.
16. J. Shin, C. Andreas Hutomo, J. Kim, J. Jang and C. Beum Park, *Natural pollen exine-templated synthesis of photocatalytic metal oxides with high surface area and oxygen vacancies*, Appl. Surf. Sci. 599 (2022), pp. 154064.
17. L.M. Hemmingsen, N. Škalko-Basnet and M.W. Jøraholmen, *The expanded role of chitosan in localized antimicrobial therapy*, Mar. Drugs 19 (2021).
18. B. Wang, J. Lan, C. Bo, B. Gong and J. Ou, *Adsorption of heavy metal onto biomass-derived activated carbon: review*, RSC Adv. 13 (2023), pp. 4275–4302.
19. C.B.D. Marien, C. Marchal, A. Koch, D. Robert and P. Drogui, *Sol-gel synthesis of TiO2 nanoparticles: effect of Pluronic P123 on particle's morphology and photocatalytic degradation of paraquat*, Environ. Sci. Pollut. Res. 24 (2017), pp. 12582–12588.
20. M. Ulfa, C. Nur and N. Amalia, *Fine-tuning mesoporous silica properties by a dual-template ratio as TiO2 support for dye photodegradation booster*, Heliyon 9 (2023), pp. e16275.
21. M. Ulfa, I.U. Hasanah and H. Bahruji, *Understanding the regenerating capacity on photodegradation of methylene blue of titania supported mesoporous silica with the aid of gelatin-P123 as bitemplate*, Commun. Sci. Technol. 9 (2024), pp. 282–290.
22. M. Rani and U. Shanker, *Green Synthesis of TiO2 and Its Photocatalytic Activity*, 2020.
23. U. Mgwetyana, M.E. Makhatha, M. Mamo and P. Ndungu, *Synthesis And Characterization Of Mesoporous Titania Using A Synthetic (Pluronic P123) And A Natural (Gum Arabic) Templating Agent*, Mater. Today Proc. 5 (2018), pp. 10585–10591.
24. *Rose petal and P123 dual-templated macro-mesoporous TiO2 for a hydrogen peroxide biosensor*. 2018.
25. M. Alijani and B.K. Kaleji, *Optical and structural properties of TiO2 nanopowders with Ce/Sn doping at various calcination temperature and time*, Opt. Quantum Electron. 49 (2017), pp. 1–16.
26. *Mesoporous TiO2 with wormlike structure synthesized via interfacial surfactant assisted route*. 2005.
27. C. Byrne, R. Fagan, S. Hinder, D.E. McCormack and S.C. Pillai, *New approach of modifying the anatase to rutile transition temperature in TiO2 photocatalysts*, RSC Adv. 6 (2016), pp. 95232–95238.
28. M. Mahalakshmi and A. Professor, *The synthesis and optical properties of TiO 2 thin film by Chemical Bath Deposition (CBD) method*, 13 (2014), pp. 424–427.
29. U. Nwankwo, R. Bucher, A.B.C. Ekwealor, S. Khamlich, M. Maaza and F.I. Ezema, *Synthesis and characterizations of rutile-TiO2 nanoparticles*

derived from chitin for potential photocatalytic applications, Vacuum 161 (2019), pp. 49–54.

30. A. Beagan, K. Alotaibi, M. Almakhlafi, W. Algarabli, N. Alajmi, M. Alanazi et al., *Amine and sulfonic acid functionalized mesoporous silica as an effective adsorbent for removal of methylene blue from contaminated water*, J. King Saud Univ. - Sci. 34 (2022), pp. 101762.
31. B. Srikanth, R. Goutham, R. Badri Narayan, A. Ramprasath, K.P. Gopinath and A.R. Sankaranarayanan, *Recent advancements in supporting materials for immobilised photocatalytic applications in waste water treatment*, J. Environ. Manage. 200 (2017), pp. 60–78.
32. C.H.A. Tsang, K. Li, Y. Zeng, W. Zhao, T. Zhang, Y. Zhan et al., *Titanium oxide based photocatalytic materials development and their role of in the air pollutants degradation: Overview and forecast*, Environ. Int. 125 (2019), pp. 200–228.
33. M.L.V.P. Chippada, B.B.V. Sailaja, T. Siva Rao, G. Divya, S.R. Nayak, B.S. Manogna et al., *Structural modification of nano titania by doping with Barium and Copper – Impact on photocatalysis: Applications in degradation of dye and pathogens*, Hybrid Adv. 3 (2023), pp. 100033.
34. M. Liu, F. Yu, L. Niu and H. Chi, *Advances in nano fi ltration membrane pore size adjustment techniques : A review*, Environ. Funct. Mater. (2025).
35. G. Zerjav, K. Zizek, J. Zavasnik and A. Pintar, *Brookite vs. rutile vs. anatase: What's behind their various photocatalytic activities?*, J. Environ. Chem. Eng. 10 (2022).
36. S.C. Padmanabhan, S.C. Pillai, J. Colreavy, S. Balakrishnan, D.E. McCormack, T.S. Perova et al., *A simple sol - Gel processing for the development of high-temperature stable photoactive anatase titania*, Chem. Mater. 19 (2007), pp. 4474–4481.
37. E.K. Moore, A. Ostroverkhova, D. Hummer, S. Morrison, Y. Peralta and S.J. Spielman, *The influence of oxygen and electronegativity on iron mineral chemistry throughout Earth's history*, Precambrian Res. 386 (2023).
38. F. Dalto, I. Kuźniarska-Biernacka, C. Pereira, E. Mesquita, O.S.G.P. Soares, M.F.R. Pereira et al., *Solar light-induced methylene blue removal over TiO2/AC composites and photocatalytic regeneration*, Nanomaterials 11 (2021).
39. V.R. Chelli, S. Chakraborty and A.K. Golder, *Ag-doping on TiO2 using plant-based glycosidic compounds for high photonic efficiency degradative oxidation under visible light*, J. Mol. Liq. 271 (2018), pp. 380–388.
40. Y. Li, Z. Ren, Z. He, P. Ouyang, Y. Duan, W. Zhang et al., *Crystallinity-defect matching relationship of g-C3N4: Experimental and theoretical perspectives*, Green Energy Environ. 9 (2024), pp. 623–658.
41. A. Soleimani-Gorgani, H.E. Al-Hazmi, A. Esmaeili and S. Habibzadeh, *Screen-printed Sn-doped TiO2 nanoparticles for photocatalytic dye removal from wastewater: A technological perspective*, Environ. Res. 237 (2023), pp. 117079.
42. O.L. Stroyuk, O.Y. Rayevska, V. V. Shvalagin, S.Y. Kuchmiy, D. V. Bavykin, E.A. Streltsov et al., *Gelatin-templated mesoporous titania for photocatalytic air treatment and application in metal chalcogenide nanoparticle-sensitized solar cells*, Photochem. Photobiol. Sci. 12 (2013), pp. 621–625.